Selective Scan Driver for Low-Power Consumption Using Oxide Thin Film Transistors

Jae-Hee Jo, Won-Been Jeong, Yu-Seong Joung, and Seung-Woo Lee, *Senior Member, IEEE*

***Abstract*— In this letter, a scan driver circuit that can generate scan signals only in a selected area is proposed. It refreshes only the area that needs to be updated without refreshing the whole display. The proposed circuit with ten stages was fabricated using oxide thin film transistors. The additional area for selective driving occupies only 14.5 % of the unit stage area. This study confirms that the power consumption in the data lines and pixels for a dot pattern can be reduced by 25 % and 37.5 % when 50 % and 25 % of scan lines are selected, respectively.**

***Index Terms*— Scan driver, oxide thin film transistor (TFT), adaptive frequency, low power display.**

I. Introduction

HIGH refresh rates have become one of the main factors in display devices as people prefer smoother motion changes [1]. However, a higher refresh rate requires more power. So, it has been difficult to apply the high refresh rate driving to mobile devices due to the limited battery time. Meanwhile, with the development of oxide thin film transistors (TFTs), low refresh rates have also become possible [2], [3]. Unlike low temperature polycrystalline silicon (LTPS) TFTs, oxide TFTs have an ultra-low leakage current characteristic [4]–[8]. It means pixel voltage is maintained for a very long time without refreshing.

To achieve both high performance and efficient power consumption, a new driving method that changes the refresh rate depending on display contents has emerged [9]. Not all contents need high refresh rates. For example, high refresh rates are not necessary when reading text messages. On the other hand, the higher refresh rate is better when watching videos such as sports games. Therefore, if the display can vary its refresh rate depending on the content, power consumption can be optimized without sacrificing the performance of the display.

Manuscript received 2 June 2022; accepted 15 June 2022. Date of publication 20 June 2022; date of current version 26 July 2022. This work was supported in part by the Technology Innovation Program (20016317, On-Panel Circuit Integration and Driving System Technology for 1270 ppi Low-Power OLED Display Based on Oxide Semiconductor) funded by the Ministry of Trade, Industry & Energy (MOTIE, Korea). The review of this letter was arranged by Editor S. Hall. *(Corresponding author: Seung-Woo Lee.)*

The authors are with the Department of Information Display, Kyung Hee University, Dongdaemun-gu, Seoul 02447, South Korea (e-mail: seungwoolee@khu.ac.kr).

Color versions of one or more figures in this letter are available at https://doi.org/10.1109/LED.2022.3184337.

Digital Object Identifier 10.1109/LED.2022.3184337

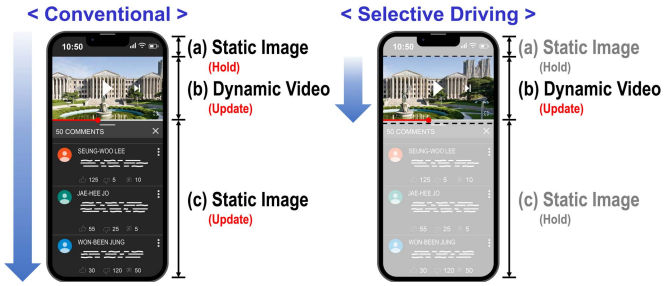

Fig. 1. A schematic diagram comparing conventional driving and proposed selective scan driving.

However, not all cases are suitable for the content-based refresh rate control technique. As shown in the example of Fig. 1, there is a complex case where dynamic video and static images are displayed simultaneously. In this case, the conventional display cannot optimize its refresh rate by contents. Because the conventional scan driver circuit sequentially generates scan signals from the first line to the last one. Even if there is no change in areas (A) and (C) in Fig. 1, unnecessary updates are needed to update the area (B). In other words, unnecessary power is wasted in areas (A) and (C) because of the high refresh rate for area (B).

Fig. 1 shows the concept of our proposed selective scan driving. Scan signals are generated only in the selected area. In the area where scan signals are not generated, pixels hold the previous frame data. Thus, it is possible to save the power consumption of the data drivers because they don't need to charge or discharge data lines and pixels by holding data voltages at the timings for the unselected areas.

In this letter, we propose a scan driver circuit that can generate scan signals only in the selected area. We can select an arbitrary area to refresh by only adding a simple memory unit comprising three transistors and one capacitor (3T1C). We will show fabrication results of the proposed circuit with ten stages using oxide TFTs.

II. Proposed Circuit

Owing to the low leakage current, oxide TFT memories and their applications have been studied [10]–[13]. Fig. 2(a) shows our proposed scan driver circuit. We add a simple memory unit comprising 3T1C to a scan driver circuit. There are two additional signals for the proposed memory unit. OE determines whether the input of the scan driver unit is connected to the previous stage or not. V_{DATA} is used for both programming and the start signal for the arbitrarily selected

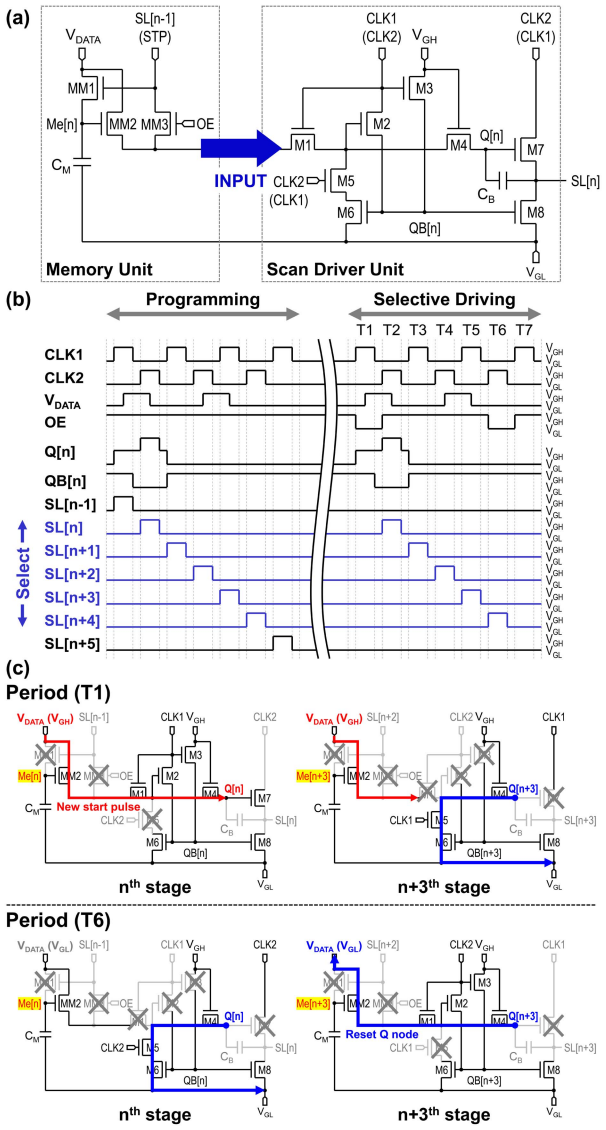

Fig. 2. (a) Circuit diagram, (b) timing diagram, and (c) detailed operation of proposed scan driver circuit.

area. The output of the memory unit is connected to the input node of the scan driver unit. Although we use a typical type of scan driver circuit [14], the proposed memory unit is also compatible with other types.

Fig. 2(b) shows a timing diagram of the proposed circuit. It represents an example of driving five stages ([n]–[n+4]) selectively. The operation principle is described as follows:

A. Programming Period

After the start pulse (STP) is generated, scan signals are sequentially generated from the first to the last stage. As shown in Fig. 2(a) and 2(b), OE keeps high (V_{GH}) in this period so that the previous output signal can be the input to the scan driver unit via MM3. The previous output signal turns on the transistor MM1 of the current stage. In Fig. 2(b) V_{DATA} goes high when SL[n-1] and SL[n+2] are high. Thus, high voltage (V_{GH}) is stored in Me[n] and Me[n+3]. The former is for the start and the latter is for the end of the selective scan.

B. Selective Driving Period

Fig. 2(c) illustrates detailed operation of the two stages where V_{GH} voltage is stored in the Me nodes. Unlike the programming period, there is no STP during the selective driving period. Instead, V_{DATA} is applied as a new start pulse via MM2 in the two stages, stages [n] and [n+3], during period T1. However, the high voltage of V_{DATA} is not transferred to Q[n+3] but to Q[n] because only CLK1 is high during period T1 as illustrated in Fig. 2(c). For this reason, the high voltage must be stored in two Me nodes of two stages where the clock connections are different. Thus, the total number of the selected scan lines becomes odd. Note that OE turns off MM3 to prevent the input node from being discharged by the previous scan line.

In period T6, OE turns off MM3 to prevent the last scan signal (SL[n+4] in Fig. 2(b)) from propagating to the next stage, SL[n+5]. However, it also prevents the Q[n+3] node from being discharged through MM3. Instead, Q[n+3] is discharged by V_{DATA} via MM2, as shown in Fig. 2(c). For this, the V_{GH} voltage must be stored in the memory node Me[n+3] during the programming period. As shown in Fig. 2(b), the last scan line is SL[n+4], but the high voltage is stored in Me[n+3] to specify the end position.

III. Results and Discussion

To evaluate the performance of the proposed circuit, we fabricated the proposed scan driver circuit with ten stages using the oxide TFTs. Fig. 3(a) represents the cross-section view of a fabricated oxide TFT with a top gate and a coplanar structure. Fig. 3(b) shows the measured transfer characteristics of the fabricated oxide TFT. The channel width and length of the TFT were 3.2 μm and 3 μm, respectively. Its threshold voltage was about −0.96 V, which means TFT operates in depletion mode. Fig. 3(c) shows the micrograph of the fabricated circuit. The area of a unit stage was 300 μm × 40 μm. The additional area for selective driving occupies only 14.5 % of the unit stage area.

Fig. 4 shows the results of the selective driving for three selected scan lines. We assumed the display has a resolution of 1080 × 1920. Refresh rates of the selected area and the rest are 120 Hz and 60 Hz, respectively. The pulse width was set to 4 μs to meet the target specification. The combination of the control signals (OE and V_{DATA}) selects scan lines with a higher refresh rate during the selective driving period. However, MM1 is slightly turned on even when V_{GS} is 0 V because V_{TH} is below 0 V. To prevent leakage of the stored data voltage, the low voltage of V_{DATA} was adjusted as much as the threshold voltage (about 1 V). As a result, scan signals were successfully generated in the selected stages highlighted in blue. The rise and fall times of the measured output waveform were 1 μs and 0.55 μs, respectively.

We investigated how much the proposed selective scan driving method can reduce power consumption. Fig. 5 shows an operation example of proposed driving method and the estimated power consumption according to the number of selected lines. A dot pattern that requires the highest dynamic power was used for estimation. The dynamic power of the proposed scan driver (P_{scan}) is dissipated in scan lines (P_{SL})

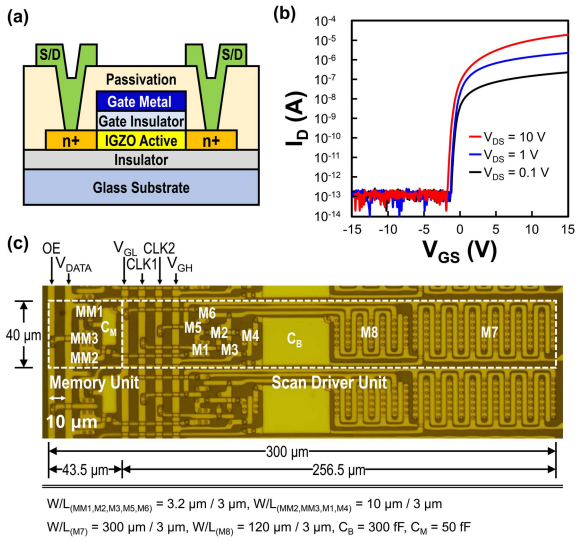

Fig. 3. (a) Cross-section view and (b) measured transfer characteristics of fabricated Oxide TFT (W/L = 3.2 μm / 3 μm). (c) Micrograph of the fabricated scan driver circuit.

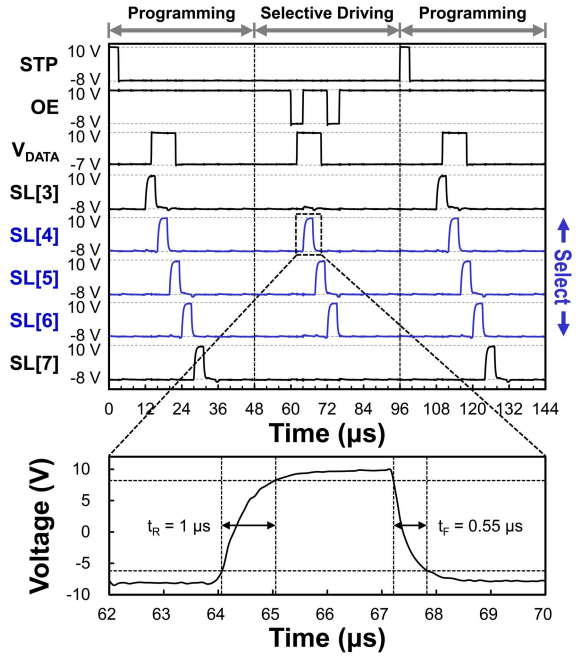

Fig. 4. Measurement results of the proposed scan driver circuit driving for three lines.

and clock lines (P_{CL}) during the selective driving period. Thus, total dynamic power can be expressed as follows:

$$\begin{aligned} P_{scan} &= P_{SL} + P_{CL} \\ &= C_{SL} \times (V_{GH} - V_{GL})^2 \times f_{frame} \times N_{stage,select} \\ &\quad + C_{CL} \times (V_{GH} - V_{GL})^2 \times f_{CLK} \times N_{stage,total} \end{aligned} \tag{1}$$

where C_{SL} and C_{CL} are the capacitance of scan lines and clock lines per unit stage. f_{frame}, f_{CLK}, $N_{stage,total}$, and $N_{stage,select}$ are frame frequency, clock frequency, the number of total stages, and the number of selected stages, respectively. Based on the fabricated circuit, the capacitance of the target specification was assumed as 25 pF and 110 fF for C_{SL}

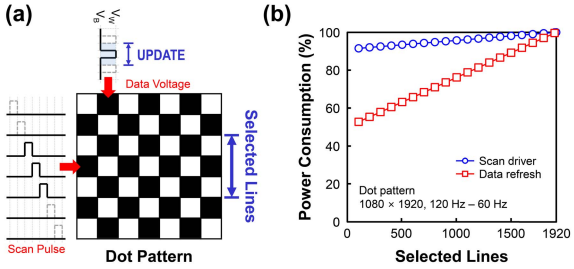

Fig. 5. (a) Operation example of the proposed driving method and (b) estimated power consumption according to the number of selected lines.

and C_{CL}, respectively. Most dynamic power is dissipated in the clock lines (P_{CL}) because the clock frequency is much higher than the frame frequency ($f_{CLK} \gg f_{frame}$). P_{CL} is independent of the number of selected lines, as shown in (1). Thus, the total dynamic power of the scan driver, depicted in blue in Fig. 5(b), changes a little according to the number of selected lines.

The dynamic power for data refreshing (P_{data}) is dissipated in pixels (P_{pixel}) and data lines (P_{DL}) during the selective driving period. Thus, total dynamic power can be expressed as follows:

$$\begin{aligned} &P_{data} \\ &= P_{pixel} + P_{DL} \\ &= C_{ST} \cdot (V_{R,W}^2 + V_{G,W}^2 + V_{B,W}^2) \cdot f_{frame} \\ &\quad \cdot (N_{stage,select} \cdot N_{DL}) + C_{ST} \cdot (V_{R,B}^2 + V_{G,B}^2 + V_{B,B}^2) \\ &\quad \cdot f_{frame} \cdot (N_{stage,select} \cdot N_{DL}) + C_{DL} \cdot ((V_{R,W} - V_{R,B})^2 \\ &\quad + (V_{G,W} - V_{G,B})^2 + (V_{B,W} - V_{B,B})^2) \cdot f_{CLK} \\ &\quad \cdot (N_{stage,select} / N_{SL}) \cdot N_{DL} \end{aligned} \tag{2}$$

where, C_{ST}, C_{DL}, and N_{DL} are the capacitance of storage capacitor, data line capacitance, and the number of data lines, respectively. $V_{R,W}$, $V_{G,W}$, $V_{B,W}$ and $V_{R,B}$, $V_{G,B}$, $V_{B,B}$ are the data voltages of RGB sub-pixels for white and black images, respectively. The dynamic power in pixel (P_{pixel}) is consumed only in selected pixels, not in the others. Moreover, as shown in Fig. 5(a), data voltages are updated only when a scan pulse is applied and remain constant for the rest of the period, which reduces dynamic power dramatically as the number of selected lines decreases. As a results, the dynamic power consumption for data refresh can be reduced by 25 % and 37.5 % when 50 % and 25 % of scan lines are selected, respectively. Thus, the proposed circuit mainly reduces the dynamic power required for unnecessary data refresh.

IV. Conclusion

In this letter, we have proposed a new scan driver circuit using oxide TFTs, which can generate scan signals only in the selected area. By reducing unnecessary refresh, it is possible to save wasted power. We added an extra memory unit to the scan driver circuit for selective driving. The additional area occupies only 14.5 % of the unit stage area, and it is also compatible with other types of scan drivers. We expect that the proposed circuit can contribute to a longer battery usage time for mobile devices by optimizing power consumption while maintaining high performance.

REFERENCES

[1] S. S. Kim, B. H. You, H. Choi, B. H. Berkeley, D. G. Kim, and N. D. Kim, "World's first 240 Hz TFT-LCD technology for full-HD LCD-TV and its application to 3D display," in *SID Int. Symp. Dig. Tech. Papers*, Jun. 2012, vol. 40, no. 1, pp. 424–427, doi: 10.1889/1.3256805.

[2] T.-K. Chang, C.-W. Lin, and S. Chang, "LTPO TFT technology for AMOLEDs," in *SID Int. Symp. Dig. Tech. Papers*, Jun. 2019, vol. 50, no. 1, pp. 545–548, doi: 10.1002/sdtp.12978.

[3] R. Yonebayashi, K. Tanaka, K. Okada, K. Yamamoto, K. Yamamoto, S. Uchida, T. Aoki, Y. Takeda, H. Furukawa, K. Ito, H. Katoh, and W. Nakamura, "High refresh rate and low power consumption AMOLED panel using top-gate n-oxide and p-LTPS TFTs," *J. Soc. Inf. Display*, vol. 28, no. 4, pp. 350–359, Apr. 2020, doi: 10.1002/jsid.888.

[4] S. Amano, H. Harada, K. Akimoto, J. Sakata, T. Nishi, K. Moriya, K. Wakimoto, J. Koyama, and S. Yamazaki, "Low power LC display using In-Ga-Zn-oxide TFTs based on variable frame frequency," in *SID Int. Symp. Dig. Tech. Papers*, May 2010, vol. 41, no. 1, pp. 626–629, doi: 10.1889/1.3500548.

[5] M. Mativenga, D. Geng, and J. Jang, "Oxide versus LTPS TFTs for active-matrix displays," in *SID Int. Symp. Dig. Tech. Papers*, Jun. 2014, vol. 45, no. 1, pp. 1–4, doi: 10.1002/j.2168-0159.2014.tb00001.x.

[6] T. Matsuo, S. Mori, A. Ban, and A. Imaya, "Advantages of IGZO oxide semiconductor," in *SID Int. Symp. Dig. Tech. Papers*, Jun. 2014, vol. 45, no. 1, pp. 83–86, doi: 10.1002/j.2168-0159.2014.tb00023.x.

[7] J.-H. Ye, C.-L. Huang, M.-Y. Chen, P.-M. Chen, K.-Y. Huang, C.-T. Peng, W.-M. Huang, and Y.-A. Wu, "Development of crystalline IGZO and LTPS hybrid TFTs array technology," in *SID Int. Symp. Dig. Tech. Papers*, May 2017, vol. 48, no. 1, pp. 600–603, doi: 10.1002/sdtp.11710.

[8] M. H. Cho, M. J. Kim, H. Seul, P. S. Yun, J. U. Bae, K.-S. Park, and J. K. Jeong, "Impact of cation compositions on the performance of thin-film transistors with amorphous indium gallium zinc oxide grown through atomic layer deposition," *J. Inf. Display*, vol. 20, no. 2, pp. 73–80, Apr. 2019, doi: 10.1080/15980316.2018.1540365.

[9] B. You, H. Nam, and H. Lee, "Image adaptive refresh rate technology for ultra low power consumption," in *SID Int. Symp. Dig. Tech. Papers*, Aug. 2020, vol. 51, no. 1, pp. 676–679, doi: 10.1002/sdtp.13958.

[10] H. Inoue, T. Matsuzaki, S. Nagatsuka, Y. Okazaki, T. Sasaki, K. Noda, D. Matsubayashi, T. Ishizu, T. Onuki, A. Isobe, Y. Shionoiri, K. Kato, T. Okuda, J. Koyama, and S. Yamazaki, "Nonvolatile memory with extremely low-leakage indium-gallium-zinc-oxide thin-film transistor," *IEEE J. Solid-Stage Circuits*, vol. 47, no. 9, pp. 2258–2265, Sep. 2012, doi: 10.1109/JSSC.2012.2198969.

[11] S.-H. Lee, B.-C. Yu, H.-J. Chung, and S.-W. Lee, "Memory-in-pixel circuit for low-power LCDs comprising oxide TFTs," *IEEE Electron Device Lett.*, vol. 11, no. 11, pp. 1551–1554, Nov. 2017, doi: 10.1109/LED.2017.2752803.

[12] J. Kim, H.-J. Chung, and S.-W. Lee, "Multi-level memory comprising low-temperature poly-silicon and oxide TFTs," *IEEE Electron Device Lett.*, vol. 42, no. 1, pp. 42–45, Jan. 2021, doi: 10.1109/LED.2020.3037059.

[13] J.-H. Jo, W.-R. Lee, H.-J. Chung, and S.-W. Lee, "A self-refreshing memory-in-pixel comprising low temperature poly-silicon and oxide TFTs for 3-bit liquid crystal displays," *IEEE Electron Device Lett.*, vol. 42, no. 6, pp. 839–842, Jun. 2021, doi: 10.1109/LED.2021.3074678.

[14] J.-H. Kim and M.-K. Woo, "Scan driver and related display apparatus," U.S. Patent 10 373 564, Aug. 6, 2019.